Bulletin of Engineering Geology and the Environment (2024) 83:244
https://doi.org/10.1007/s10064-024-03742-6

ORIGINAL PAPER

Experimental assessment of channel narrowness effects on debris-flow erosion

Lan Ning[1,2] · Kaiheng Hu[1] · Pu Li[1] · Haiguang Cheng[1,2] · Qiyuan Zhang[1]

Received: 28 January 2024 / Accepted: 29 April 2024

Abstract
An in-depth understanding of debris flow erosion is crucial for estimating debris flow magnitude and evaluating its risk. Although the mechanisms of debris flow erosion have been widely explored by previous studies, channel downcutting and lateral erosion of debris flows over irregular erodible beds are still poorly understood. Here, we investigate the debris flow erosion characteristics in non-uniform erodible beds with variable cross-sections based on a series of small-scale flume experiments. We quantify the effects of debris flow density, bed slope, bed fine particle content, and channel narrowness on downcutting and lateral erosion. Downcutting Erosion Depths (DED) first increased linearly with the debris-flow density and bed slope; however, it exhibited a decrease afterward and an increasing trend with the narrower channel. The maximum DED was observed when the channel narrowness was 0.7. Similarly, a total erosion efficiency was introduced to measure the intensity of debris flow erosion. The efficiency increased linearly with the flume slope and decreased with the fine particle content of the bed and debris flow density. On the other hand, the efficiency grew exponentially with the channel narrowness. A dimensionless parameter, defined as the ratio of downward erosion to lateral erosion, was utilized to assess the relative importance of the downward and lateral erosion of the debris flow. Experimental results show that the ratio is positively correlated with debris flow density and flume slope. Notably, the effect of bed fine particle content was relatively weak, and downward erosion overwhelmed lateral erosion for significant channel narrowing. Furthermore, the ratio increased logarithmically with the channel narrowness, whereas the lateral erosion exceeded the downward erosion for smaller narrowness and vice versa. Our experimental results demonstrate that the amount and mechanism of debris flow erosion may differ significantly in irregular erodible beds.

Keywords Debris flow · Narrowing erosion · Erosion efficiency · Downcutting erosion rate · Lateral spreading rate

Introduction

Large-scale landslides triggered by earthquakes or rainstorms in alpine valleys deposit huge volumes of soils and rocks in their channels that significantly alter the channel morphology and are the potential sediment source for subsequent debris flows (Whipple and Dunne 1992; Zhang and Zhang 2017; Zhang et al. 2019). Previous research has shown that a narrow channel obstructed by a landslide dam can significantly enhance the sediment transport capacity (Croissant et al. 2017) For instance, several narrow sections in the channel significantly intensified the debris flow erosion during the 2010 Zhouqu and 2022 Meilong debris flow (Ning et al. 2022; Hu et al. 2011).

Several studies have discussed the lateral erosion phenomena due to debris flow (Al-Riffai 2014; Lyu et al. 2017). Lateral erosion increases both the density and frictional resistance of the debris flow (Berti et al. 1999; Breien et al. 2008; Godt and Coe 2007). The continuous change in debris flow density frictional resistance (Hungr et al. 2005) increases or decreases debris flow velocity (Mangeney et al. 2010). Numerous studies have also discussed the process of downward erosion (Breien et al. 2008; Godt and Coe 2007; Li et al. 2018). Several variables, including debris flow depth(Berger et al. 2011; Schürch et al. 2011), bed slope (Theule et al. 2015), shear stress (Berger et al.

✉ Kaiheng Hu
khhu@imde.ac.cn

1 Institute of Mountain Hazards and Environment, Chinese Academy of Sciences, No.189 of Qunxiannanlu Street, Chengdu 610041, Sichuan, China

2 University of Chinese Academy of Sciences, Beijing 100049, China

Published online: 23 May 2024

2011; Han et al. 2015a, b; Schürch et al. 2011), particle collision stress(Han et al. 2015a, b), and the water content (Iverson et al. 2011) are positively correlated with the rate of downward erosion. Meanwhile, debris flow erosion also plays a critical role in increasing the volume of debris flow and changing the properties of debris flow, such as density, rheology, and flow velocity (Berti and Simoni 2005; Hungr et al. 2005, 1984; Iverson 1997; McDougall and Hungr 2005), which significantly increases the instability and destructiveness of debris flow (Lyu et al. 2018).

Field observations of debris flows can be highly challenging due to their instability and destructive nature. Therefore, flume tests have become essential for studying debris flow erosion (De Haas et al. 2015; De Haas and Van Woerkom 2016; Egashira and Ashida 1987; Hsu et al. 2008). However, current flume tests often simulate debris flows for constant bed width. This approach, while informative, may overlook a key factor in the natural dynamics of debris flows— the effect of narrowing erodible beds. As channels experience changes in width, it can impact flow velocity, shear stress, and the overall erosive potential of debris flows (Hu et al. 2013). Ignoring these dynamic bed width variations may limit the realism of flume experiments and hinder a comprehensive understanding of debris flow erosion.

Our study aims to investigate erosional mechanisms when debris flows pass through narrowing erodible beds. Specifically, we aim to identify and quantify the influences of channel narrowness, bed fine particle content, bed slope, and debris flow density on debris flow erosion. During the experiment, we recorded vital parameters, such as flow velocity, depth, and DED, as the debris flow passed over the narrowing erodible beds. This enabled us to quantify the impact of bed narrowing on DED and erosion efficiency. Additionally, we have introduced a crucial dimensionless parameter (ξ) to assess the relative importance of the downward and lateral erosion of the debris flow. This parameter will provide a clear understanding of the dynamic process of debris flow under varying channel narrowness, particularly focusing on erosion behavior in different directions.

Materials and methods

Experimental setup

Experiments were conducted in a 7.0 m long, 0.6 m wide, and 1.0 m high flume with an erodible, unsaturated, and loosely packed unconsolidated bed (Fig. 1). The downstream part functioned as a reservoir with a volume of 1.2 m^3 for gathering tail debris flow. Likewise, the experimental flume in the middle comprised a fixed bed of 2 m and an erodible bed of 5 m. The fixed bed aimed to stabilize the flow and reduce turbulent inflow. The sediment thickness in the erodible bed segment was 0.3 m and maintained a uniform slope. The thickness of the erodible bed had been designed to be greater than the maximum depth to be entrained in all cases. A gently sloping section with varying widths was integrated into the erodible bed, which was 0.3 m high. The ratio of the cross-sectional area of the loose accumulations in the bed to the total area of the bed was defined as channel narrowness (*k,* which is defined as shown in Fig. 1d). The corresponding *k* values were 0, 0.25, 0.4, 0.55, and 0.7, indicating different lateral constrictions (Fig. 1d).

The shape of the bed also impacts the flow characteristics of the debris flow in the experiments (Lyu et al. 2017). The geometry of the bed included one sloping bank while the other coincided with the vertical glass flume wall. For simplicity, the frictional resistance near both banks of a channel was assumed to be the same. The glass sidewalls, often with smooth surfaces, did not play a significant role in the flow dynamics (Lyu et al. 2017; Han et al. 2015a, b). Since flow resistance near the glass sidewalls is usually lower than that of natural banks, the longitudinal velocity distribution near the glass sidewalls represented the velocity along the longitudinal centerline in our case. Even though several limitations related to this geometry might have influenced the debris flow features, this approach was believed to apply to the erosion analysis when debris flows pass through a narrow section in the bed (Lyu et al. 2017).

Material composition

The debris flow material and the bedding soil on the flume were obtained from undisturbed soil samples from Jiangjia gully that had undergone screening. The debris flow material was sieved through a 2 cm mesh. Subsequently, the soil was mixed with water to a volume of 0.3 m3, according to the established density. The well-mixed debris flow was then placed in the hopper. The particle size distribution curve for the undisturbed soil of Jiangjia gully was obtained from the particle analysis experiment (Fig. 2). Considering the limitations of the Jiangjia gully undisturbed soil and actual site conditions for the bed soil, we maintained a fixed (20%) percentage of coarse particles (10–20 mm) in the bed soil, while changed the content of particles with a diameter less than 2 mm (d < 2 mm), subsequently altering the ratio of clay particles (d < 0.005 mm). The straight shear test resulted in a soil friction angle of 30°.

Experimental instrument

A digital camera (Panasonic, named camera 1) with a resolution of 1440 × 1080 pixels and a frame rate of 25 frames per second (fps) was installed at the top of section AB to record the debris flow front kinetics (Fig. 2). A second digital camera with the same resolution and fps (denoted as camera 2)

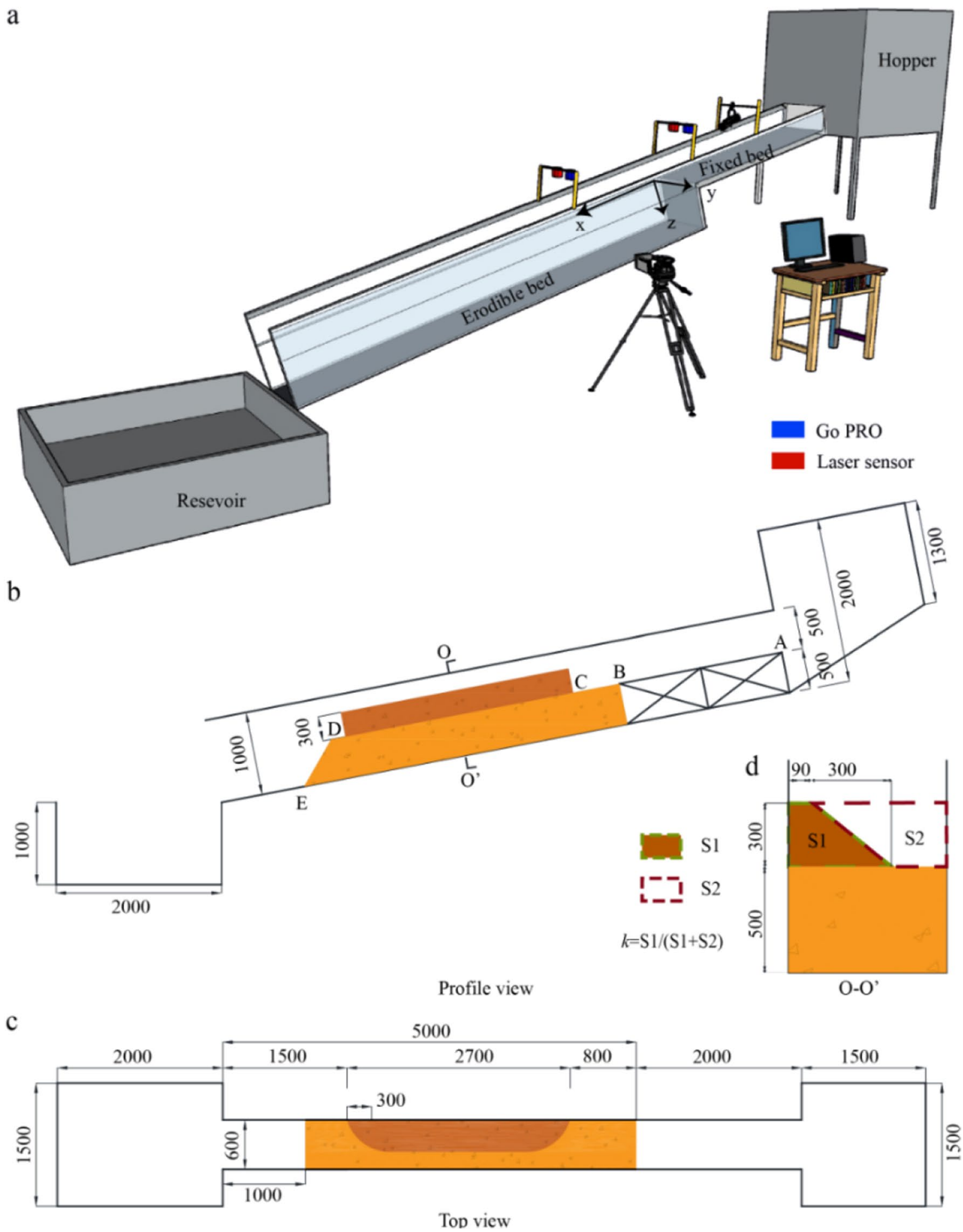

Fig. 1 (**a**) Experimental flume. (**b**) The profile view of the flume. (**c**) The top view of the flume. (**d**) O–O' profile (The diagram shows a bed with a channel narrowness of 0.4, and all numbers are in mm)

was fixed on one side of the setup to record the downward erosion process. During the experiment, two laser sensors (Leuze ODSL, named MLM 1 and 2) were used to measure the debris flow depth in sections AB and BC. The sensors had an error margin of 1 mm and a sampling frequency of 12 Hz. Two GoPros, each with a resolution of 2560*1440 pixels and a high frame rate of 240 frames, were installed at the top of sections AB and BC. The velocity for both cross-sections was obtained using PIV plugins (Particle Image Velocimetry, a MATLAB plug-in), which have several

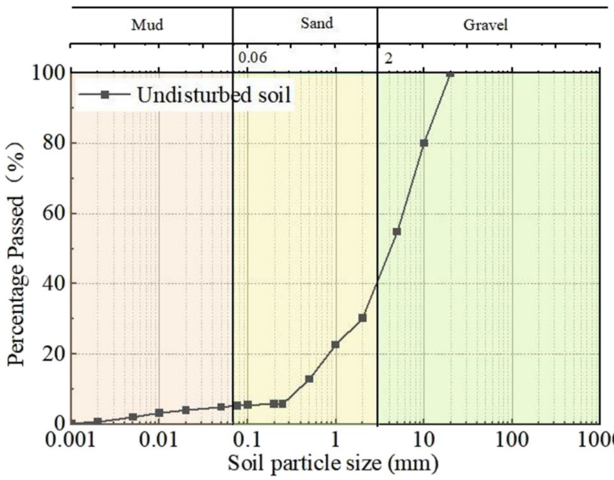

Fig. 2 Particle-size distribution of undisturbed soil in Jiangjia gully

advantages, including a wider measurement range and real-time capabilities—compared to traditional methods.

Experimental procedure and data analysis

Flume experiments were conducted for 45 different cases with varying parameters, including debris flow density (ρ), bed slope (S), bed fine particle content (w), and channel narrowness (k). We selected three bulk density values (1.5, 1.7, and 1.9) to represent dilute, sub-viscous, and viscous debris flows observed in nature (Jakob et al. 2005). Slopes of 8°, 11°, and 14° were chosen, where 8° represents the accumulation fan slope, 14° the circulation zone slope, and 11° an intermediate slope. Additionally, we analyzed accumulation deposit geometries in debris flow catchment and selected channel narrowness values of 0, 0.25, 0.4, 0.55, and 0.7. Bed fine particle content was varied from 0 to 45% at equal intervals of 15% to assess its impact on debris flow erosion under typical study conditions. A summary of the variables from all experiments is shown in Table 1. For each case, two tests were conducted to account for the effects of natural variability. In each test, the debris flow was continuously agitated with a stirrer before releasing from the flume outlet to prevent consolidation and phase separation. During each test, the hopper outlet was raised for 1 s, triggering the data acquisition system that consisted of each pair of digital cameras, GoPros, and laser sensors. The PIV plug-in calculated the debris flow velocity (Patalano 2017). The computed velocity's reliability depended on the image's quality, so we adjusted the image by comparing it to reduce the errors (Gao 2006). DED was measured by placing colored sand markers. The markers were placed at 20 cm intervals vertically and 10 cm intervals horizontally. After the debris flow, we measured DED by determining the remaining

Table 1 Experimental parameters for each group

Test ID	Debris flow density ρ (g/cm^3)	Channel narrowness k (-)	Fine particle content of the bed w (%)	Slope S (°)
$ND_{1, 2, 3}$-a	1.5, 1.7, 1.9	0	0	11
$ND_{1, 2, 3}$-b	1.5, 1.7, 1.9	0.25	0	11
$ND_{1, 2, 3}$-c	1.5, 1.7, 1.9	0.4	0	11
$ND_{1, 2, 3}$-d	1.5, 1.7, 1.9	0.55	0	11
$ND_{1, 2, 3}$-e	1.5, 1.7, 1.9	0.7	0	11
$NP_{1, 2, 3, 4}$-a	1.5	0	0, 15, 30, 45	11
$NP_{1, 2, 3, 4}$-b	1.5	0.25	0, 15, 30, 45	11
$NP_{1, 2, 3, 4}$-c	1.5	0.4	0, 15, 30, 45	11
$NP_{1, 2, 3, 4}$-d	1.5	0.55	0, 15, 30, 45	11
$NP_{1, 2, 3, 4}$-e	1.5	0.7	0, 15, 30, 45	11
$NS_{1, 2, 3}$-a	1.5	0	0	8, 11, 14
$NS_{1, 2, 3}$-b	1.5	0.25	0	8, 11, 14
$NS_{1, 2, 3}$-c	1.5	0.4	0	8, 11, 14
$NS_{1, 2, 3}$-d	1.5	0.55	0	8, 11, 14
$NS_{1, 2, 3}$-e	1.5	0.7	0	8, 11, 14

Test ID '$ND_{1,2,3}$' represents 'debris flow density ρ=1.5, 1.7,1.9 g/cm^3';

'$NP_{1, 2, 3, 4}$' represents 'fine particle content of the bed w=0, 15, 30, 45%';

'$NS_{1, 2, 3}$'represents 'channel slope S=8, 11, 14°';

In all test IDs, 'a, b, c, d, and e' represent 'channel narrowness k=0,0.25,0.4,0.55,0.7'

height of the colored sand, excluding the debris flow accumulation. Finally, the remaining width of the narrow section was determined and used to calculate the lateral spread rate. All the erosion rate data for downcutting depth or lateral erosion rate mentioned below are OO' sections (Fig. 1b).

Bed erosion by debris flow may occur when sediment is mobilized by basal shear forces (Hungr et al. 2005; Takahashi 1981). It may also be related to grain collisional stresses arising from the shear of granular material (Hsu et al. 2008; Stock and Dietrich 2006). The basal shear force exerted on the bed by the flowing mixture of debris was estimated through its shear stress (τ/Pa):

$$\tau = \rho g H \sin(S) \quad (1)$$

where ρ is debris flow density (kg/m^3), g is the gravitational acceleration (m/s^2), H is the debris flow depth (m), and S is the slope of the bed (°). We approximated the debris flow density for a thoroughly mixed flow, using the maximum flow depth as an input. Nonetheless, this introduces minor errors, as the flow depth and density are not constant over time. This is because the flow front typically develops a relatively high solids fraction.

The collisional stress (σ_{gc}/Pa) in the experimental debris flow can be calculated as follows (Hsu et al. 2008; Stock and Dietrich 2006)

$$\sigma_{gc} = v_s \rho_s D^2 \gamma^2 \tag{2}$$

where v_s is the volume solids fraction, ρ_s is the density of solid particles (kg/m^3), and D is the characteristic particle diameter (m), approximated as the median particle size of the debris flow. The shear rate y(s$_{-1}$) is defined as (Iverson 1997; Iverson et al. 1997; Savage and Hutter 1989):

$$\gamma = \frac{u}{H} \tag{3}$$

where u is the debris flow velocity (m/s). Our study's approximation of the shear rate assumes a linear vertical velocity distribution. In reality, debris flows often deviate from linearity in their vertical velocity distribution (Kaitna et al. 2014). However, due to a lack of available data on the vertical velocity distribution of the experimental debris flows presented here, we estimate the shear rate using Eq. 3.

Results

Erosion process of channel narrowing

Following the passage through the narrow section, the debris flow characteristics, including flow velocity, depth, and Froude Number (Fr), underwent alterations, impacting the erosion dynamics.

Emerging from the hopper, the debris flow traversed the upstream fixed bed segment, transitioning into a stable flow state. The debris flow movement, which induced significant erosion on the bed material, was influenced largely by the incoming flow velocity and the channel's narrowness. Our experimental findings highlighted that in the initial phases of a debris flow, the incoming flow exhibited notable strength, characterized by the high velocity at the debris flow head, resulting in turbulent and chaotic disturbed flow patterns with intense turbulence (Fig. 3). Notably, the erosion at the narrow section's front end predominantly manifested as impact erosion due to the debris flow's high-speed flow

Fig. 3 Erosion process at the front end of the narrow channel (**a**, **b**, **c**, and **d** are k = 0.15, 0.4, 0.55, and 0.7, respectively)

and vigorous impact, causing sharp impacts and abrasion on the accumulation body at the front end ($t=1.5$–2.05 s of Fig. 3a, b c and d). As the debris flow progressed, approaching a more stabilized flow state, the initial kinetic energy and impact force diminished, leading to a gradual decline in impact erosion on the accumulation body at the front end ($t=2.75$–3.55 s of Fig. 3a, b c and d). This transitional phase reveals two erosion patterns—impact and shear erosion. Impact erosion is prominent in wider channels due to the fluid's rapid flow, while shear erosion dominates in narrower channels, differing from impact erosion yet similarly converging toward stability.

Upon the debris flow entry into the middle section of the narrow channel, a distinct erosion process emerged—compared to those at the front. Illustrated in Fig. 4, the lateral erosion process in this section is exemplified using NP1-d. Initially, the debris flow swiftly advanced downstream on the lower side, causing substantial erosion of the channel material. Ongoing experimentation in which the bottom bed did not contain fine particles revealed continuous scouring and deepening of the channel, alongside recurring collapses along the higher channel side, as depicted at 1.2 s in Fig. 4. This evolution was marked by the gradual widening of the channel, characterized by the interplay between down-cut and lateral erosion. In the initial erosion phase, shear stress between debris flows governed the erosion process, with widening channel beds leading to increased height of steep thresholds and reduced bank stability. Subsequently, in the channel bank collapse stage, steep slopes formed at the bank edges due to the sole interaction of debris flow with the soil at the steep slope bottom. This interaction triggered the gravitational failure of the upper soil, predominantly observed as overturning failure at $t=3.25$ s (Fig. 4g). Significantly, the presence of fine particles in the soil influenced the channel material's erosion mechanism. Figure 5 illustrates the process of lateral erosion occurring in the middle of the narrow section under high fine particle content in the bed. Upon the start of the experiment, the debris flow rapidly flooded into the lateral accumulations, quickly saturating the surface soil. As a result of the impact and infiltration of the debris flow, the surface soil of the accumulations gradually became loose and started to peel off. With the ongoing inflow and impact of the debris flow, the peeling of the surface soil intensifies. The flow depth of the debris flow controlled this process.

Erosion depth and influencing factors

We systematically assessed the factors influencing the maximum DED of OO' profile, including the effects of channel narrowness, bed composition and slope, and debris flow density. Linear regression analyses were used to statistically assess the relationships between the maximum DED and flow velocity, debris flow depth, flume slope, debris flow density, bed fine particle content, grain collisional stress, and shear stress (Fig. 6). The results indicate a linear relationship between variables and erosion depth, but other relationships, such as exponential or logarithmic, cannot be excluded. It is important to note that the variability of debris flow, the highly variable and stochastic bed erosion processes, and the limited sample contributed to relatively weak statistical significance and relatively high *p*-values.

The maximum DED increased as the debris flow velocity, depth, bed slope, and shear stress gradually increased (Fig. 6a, b, and d). However, the relationship between grain collisional stress and maximum DED calculated from Eq. 3 shows poor correlation (Fig. 6c). Therefore,

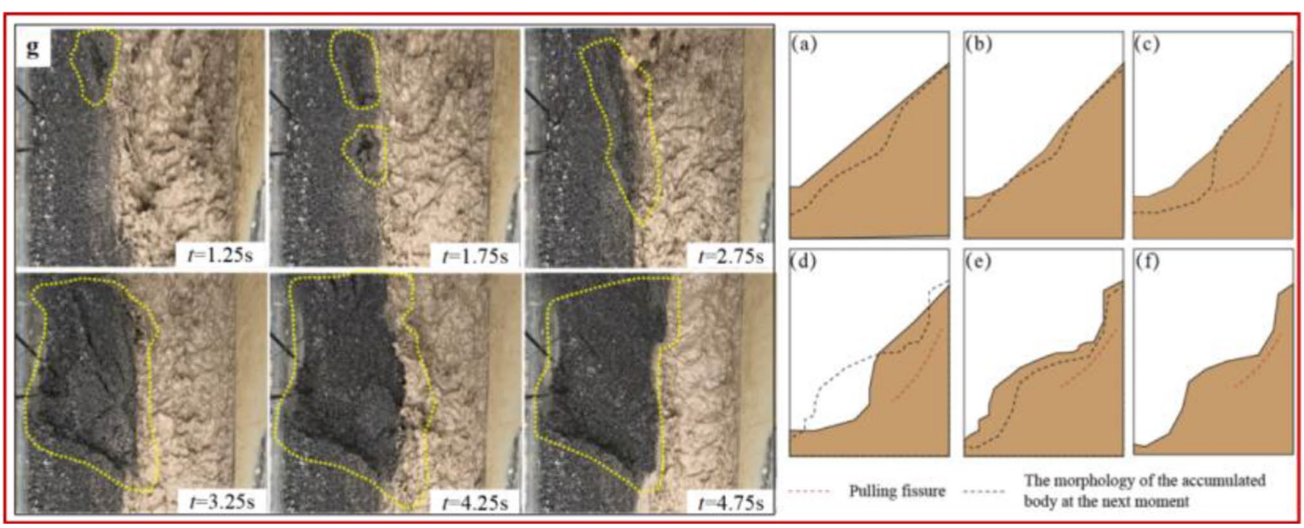

Fig. 4 Temporal variations in lateral erosion within a narrow channel section lacking fine particles (NP1-d) (**a**, **b**, **c**, **d**, **e**, **f**: Diagrams of the bed lateral erosion process without fine particles; **g**: Photos of the bed lateral erosion process without fine particles)

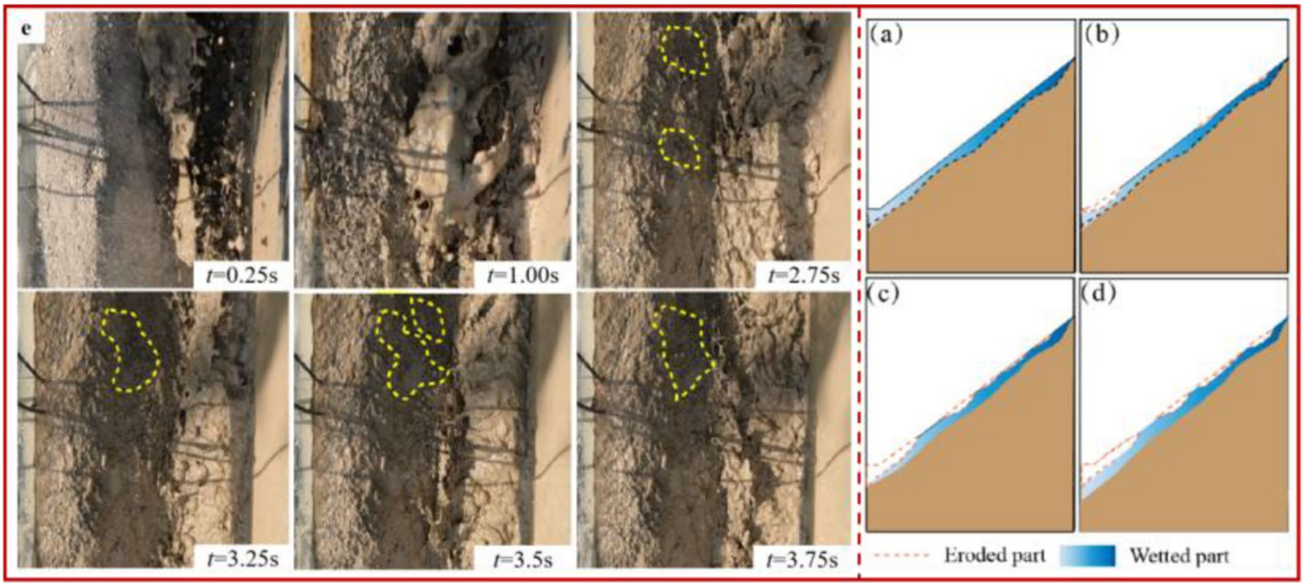

Fig. 5 Temporal variations in lateral erosion within the narrow section containing 45% fine particles (NP1-d) (**a**, **b**, **c**, **d**, **e**, **f**: Diagrams of the bed lateral erosion process with fine particles; **g**: Photos of the bed lateral erosion process without fine particles)

we carried out a detailed analysis of the relationship between erosion depth and these variables. At different channel narrowness, the DED increased significantly with the increase of debris flow velocity (Fig. 6a). The linear determination coefficient (R^2) ranged from 0.04 to 0.66, with the slope of the curve ranging from 0.1 to 2.13. We observed that R^2 was highest at a channel narrowness of 0.4 and lowest at a channel narrowness of 0.7, showing little correlation. The debris flow depth exhibited an increase with the channel narrowness. The maximum debris flow depth was 0.23 m and occurred at the channel narrowness of 0.55. As the debris flow depth increased, the erosion depth also increased significantly. However, the relationship between debris flow shear stress and DED exhibited significant scatter, with R^2 ranging from 0.11 to 0.43. As the degree of narrowing increased from 0 to 0.55, R^2 showed a gradual decrease. When the narrowing reached 0.7, R^2 attained a maximum value of 0.43 (Fig. 6d).

Previous studies have shown that slope is the main factor influencing debris flow erosion: as the slope increases, so does the depth of erosion (Borrelli et al. 2020; Breien et al. 2008; Stock and Dietrich 2006). Our experiments observed the relationship between DED and slope at different degrees of bed narrowing (Fig. 6e). The results indicate a high determination coefficient for each degree of narrowing, ranging from 0.54 to 0.98. Fitted curves can effectively explain the observed change in DED with slope. Several studies, for instance (Prochaska et al. 2008), have also mentioned that the debris flow velocity increases with the increasing slope. As mentioned above, there is a positive correlation between debris flow velocity and erosion depth (Fig. 6a).

The experiments demonstrate the critical effect of bed fine particle content on debris flow erosion (Fig. 6g). When no fine particles are present in the bed, the data points are relatively discrete. We speculate that when the fine particle content is 0, the lateral soils are more prone to collapse, preventing downward erosion. As the bed fine particle content increased from 15 to 30%, erosion decreased; nevertheless, the erosion depth increased upon further augmentation to 45%. This trend was consistent across all channel narrowness except 0.7. We infer that the anomaly is due to the convergence of the center streamlines at a more considerable channel narrowness.

Our experimental results show that with the increase of the degree of bed narrowing, DED tends to decrease first and then increase and reaches its lowest value when $k = 0.25$ and a maximum value at $k = 0.7$ (Fig. 6h). It can be explained by the shrinkage in cross-section area when the debris flows pass over narrowing erodible beds, and the corresponding in debris flow velocity and depth. At higher flow velocities and depths (Fig. 6a and b), debris flows are more likely to erode the bed. Therefore, we can establish a relationship between the channel narrowness, bed cross-sectional area, and the debris flow depth. This implies that the narrower the bed and its cross-sectional area, the higher the flow depth and the more intense the erosion.

Erosion efficiency

We defined erosion efficiency (E_s) as the sum of the downcutting erosion rate and the lateral expansion rate, which assesses the intensity of debris flow erosion, as illustrated by the formula below:

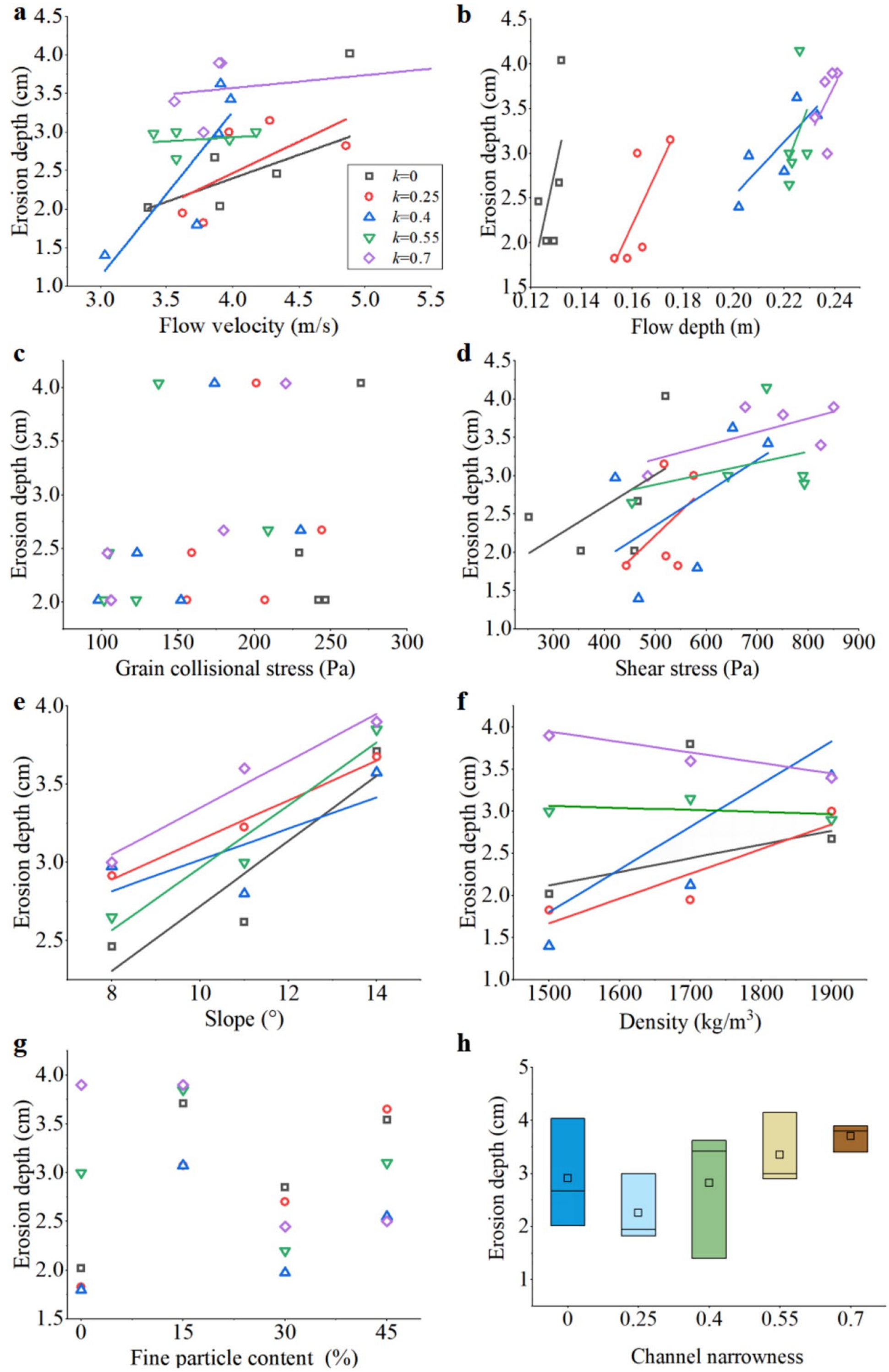

Fig. 6 Relation between the maximum erosion depth in the middle of the narrow bed and bed slope, flow velocity, flow depth, discharge, shear stress and grain collisional stress, debris flow density, bed fine particle content, and channel narrowness. (No regression lines are plotted for grain collisional stress and bed fine particle content due to the absence of a correlation)

$$E_s = E_d + E_l \tag{4}$$

where E_d is the downcutting erosion rate (cm/s); E_l is the lateral erosion rate (cm/s). The change in erosion efficiency is closely related to many factors, including bed slope, bed fine particle content, debris flow density, and channel narrowness.

An increase in bed slope leads to an increase in erosion efficiency (Fig. 7a), which can be attributed to the increases in debris flow velocity that result in deeper incisions (Fig. 6a).

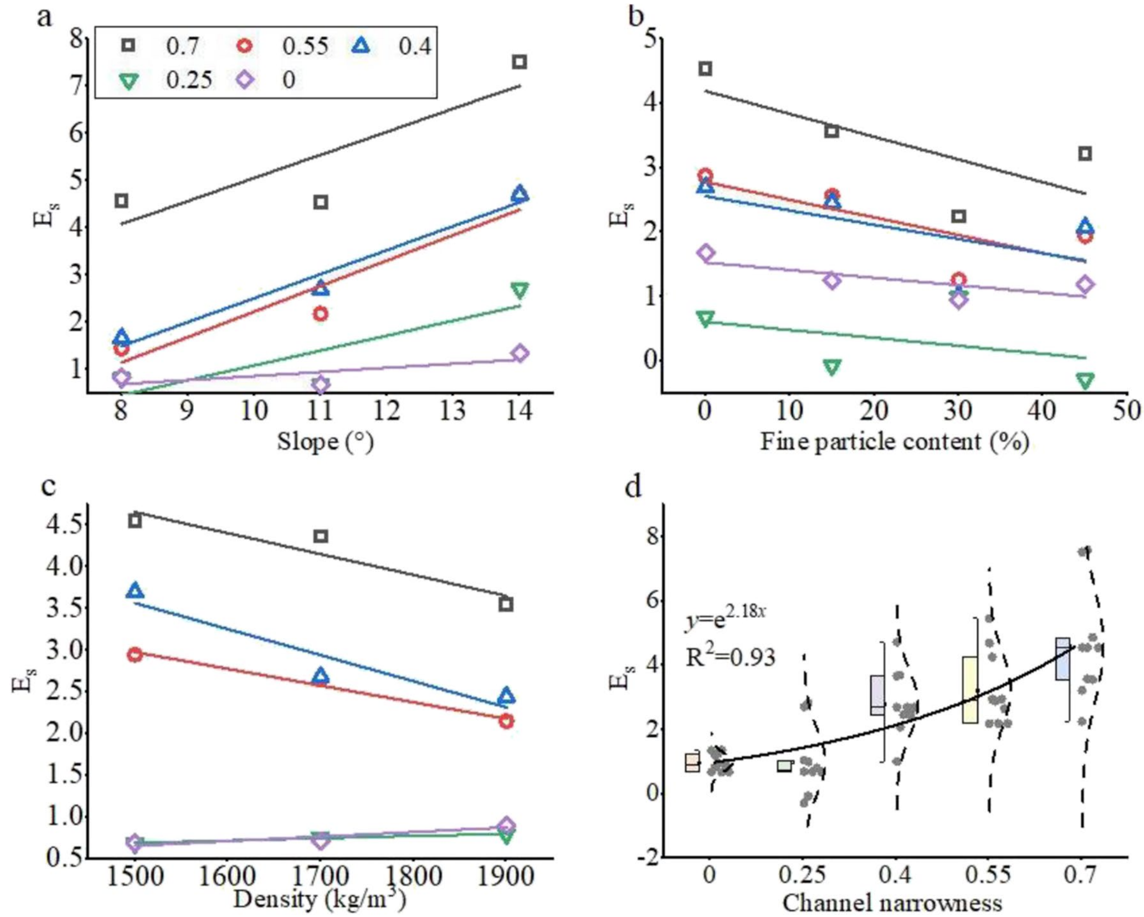

Fig. 7 The relationship between erosion efficiency and various parameters

A higher slope provides more kinetic energy for the debris flow, leading to more effective erosion. The linear regression results show that as the channel narrowness increased from 0 to 0.7, the bed slope's effect on erosion decreased. The slope had the most substantial impact on erosion at $k = 0.55$. This suggests that the enhancing effect of increasing slope on erosion is closely related to the channel narrowness.

An increase in the bed's fine particle content leads to decreased erosion efficiency. This is because the porosity gradually decreases as the bed's fine particle content increases. The smaller bed particles fill the existing pores, making them dense and slowing down erosion. Decreased porosity affects water distribution in the bed, changing the hydraulic conditions and influencing the erosion intensity. Linear regression results show that the slope of the curve decreases from -0.01 to -0.03 as the degree of narrowing increases from 0 to 0.7. With the degree of narrowing increasing from 0.25 to 0.7, the absolute slope of the fitted line decreased, ranging from -0.124 to -0.035. This suggests that the effect of bed fine particle content on debris flow gradually increases as the channel narrows. The effect is more pronounced in narrower channels, increasing the resistance to debris flow mobility and erosion.

As debris flow density increases, the suspension and movement are impeded, thus slowing the velocity and lowering the energy and erosion efficiency (Fig. 7c). The fitting results indicate that an increase in the degree of narrowing leads to higher erosion efficiency. The erosion efficiency increases exponentially with the rise in the channel narrowness (Fig. 7d). This is attributed to debris flow becoming more concentrated and rapid in the bed. The concentrated and rapid flow may enhance erosion, especially when it passes through narrow channels.

Relationship between the ratio of erosion rates and various parameters

We define a dimensionless parameter ξ that represents the ratio of the downward erosion rate to the later expansion rate as follows:

$$\xi = E_d / E_l \tag{5}$$

The purpose of this parameter is to indicate the relative importance of lateral and vertical erosion of debris flows. If $\xi > 1$, it indicates a relatively high downward erosion rate, implying more incision. If $\xi < 1$, it indicates a relatively high rate of later expansion, signifying more lateral extension. When $\xi = 1$, it indicates a relative balance between the incision rate and lateral extension rate. In this case, debris flow erosion may have similar characteristics laterally and vertically. By looking at the value of ξ, we can infer the main direction of erosion under different conditions.

In general, ξ and debris flow density have an inverse relation (Fig. 8a), suggesting that the debris flow is concentrated on a downward incision rather than expanding laterally. In our experiments, ξ is less than 1 in all cases except for $k = 0.25$, which means that debris flow is more easily to incise the bed when the channel narrowness is larger, where lateral expansion plays a leading role in less narrowing. The results of the linear fit show that as channel narrowness increases, the absolute value of the fitted curve slope decreases in larger narrowing. This suggests that the effect of debris flow density on erosion gradually decreases as the bed narrows.

As the slope increases, ξ also increases (Fig. 8b), implying a relative rise in the downward erosion as the slope becomes steeper. Debris flows in steep slopes tend to incise more strongly, possibly because the increased slope imparts more kinetic energy, leading to a more efficient downward incision along the main flow line. In addition, the linear fit shows that as the channel narrows, so does the slope of the fitted curve. It suggests that the effect of slope on ξ further enhances as the bed narrows.

The effect of bed fine particle content on ξ is comparable with debris flow density but not obvious (Fig. 8c). For minor channel narrowness ($k = 0.25$ and 0.4), the slopes of the fitted curves are negative, meaning the increasing the bed fine particle content appears to cause more lateral erosion. However, the slopes of the fitted curves are positive when the channel narrowness is greater ($k = 0.55$ and 0.7). That means the effect of fine particles on erosion gradually increases with the channel narrowness. Meanwhile, when $k = 0.25$, $\xi < 1$, signifies that lateral erosion dominates.

We also summarize the effect of the channel narrowness on ξ. It was observed that as the channel narrowness increases, ξ increases logarithmically (Fig. 8d). Consistent with the previous cases (Fig. 5a, b, and c), ξ is still less than 1 when $k = 0.25$. It suggests lateral erosion is still dominant at a small channel narrowness. However, with a further increase in the channel narrowness, ξ gradually exceeds 1, indicating that incise erosion becomes more significant at a larger channel narrowness. This emphasizes the vital effects of bed narrowing on debris flow erosion. Our experiments showed that the lateral collapse area was smaller for a large channel narrowness ($k = 0.55/0.7$)

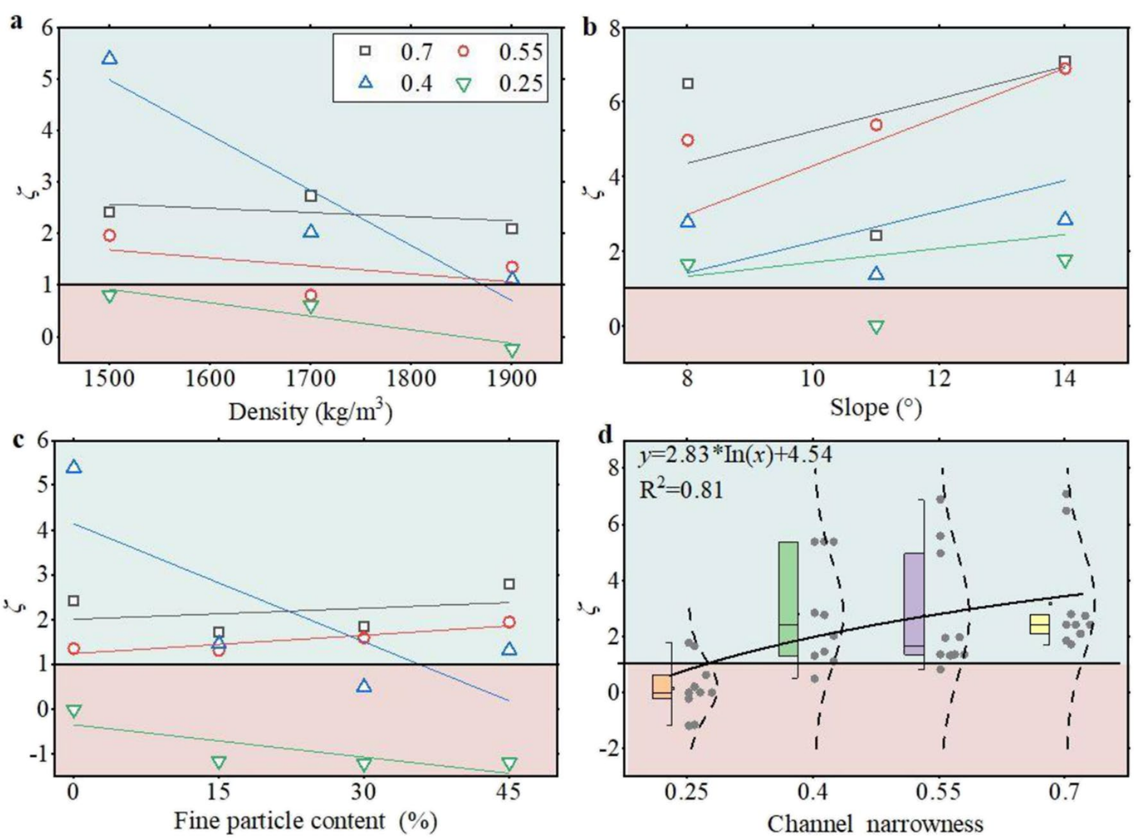

Fig. 8 The relationship between the ratio of erosion rates and various parameters (downcutting erosion rate divided by lateral spreading rate)

(Fig. 9a and b). Conversely, the lateral collapse was more pronounced, and the collapse area was larger for a small channel narrowness ($k=0.25/0.4$) (Fig. 9c and d). Additionally, the relative collapse area (the value of the actual collapse area divided by the area of the initial narrow bed part) increased with the channel narrowness (Fig. 9).

Discussion

Effects of debris flow characteristic on erosion

Our experiment demonstrates that factors such as basal shear stress, flow velocity, flow depth, bed fine particle content,

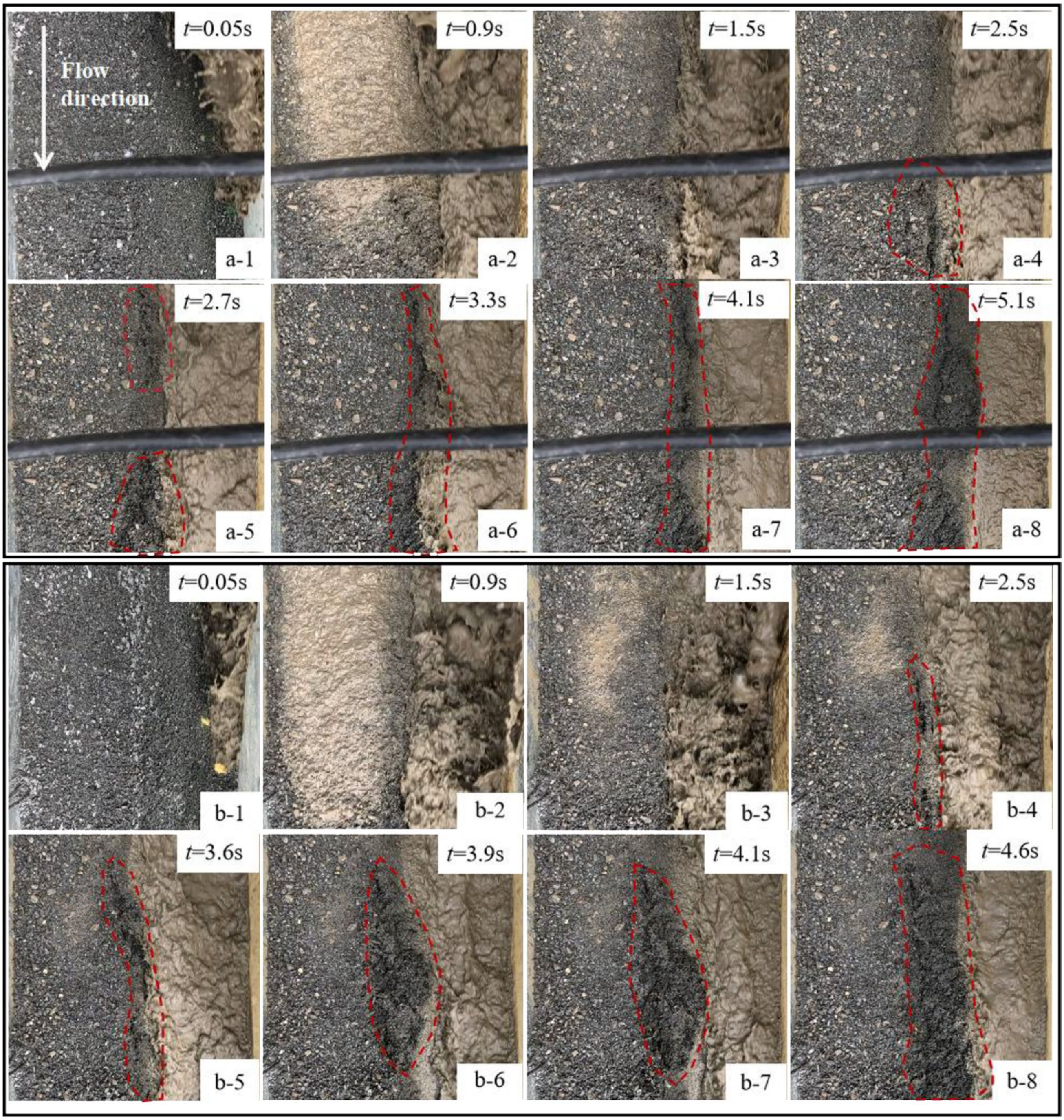

Fig. 9 Lateral erosion characteristics in the middle section of the narrowing part with time, (**a**), (**b**), (**c**), and (**d**) is the lateral erosion process when the channel narrowness is 0.7, 0.55, 0.4, and 0.25, respectively

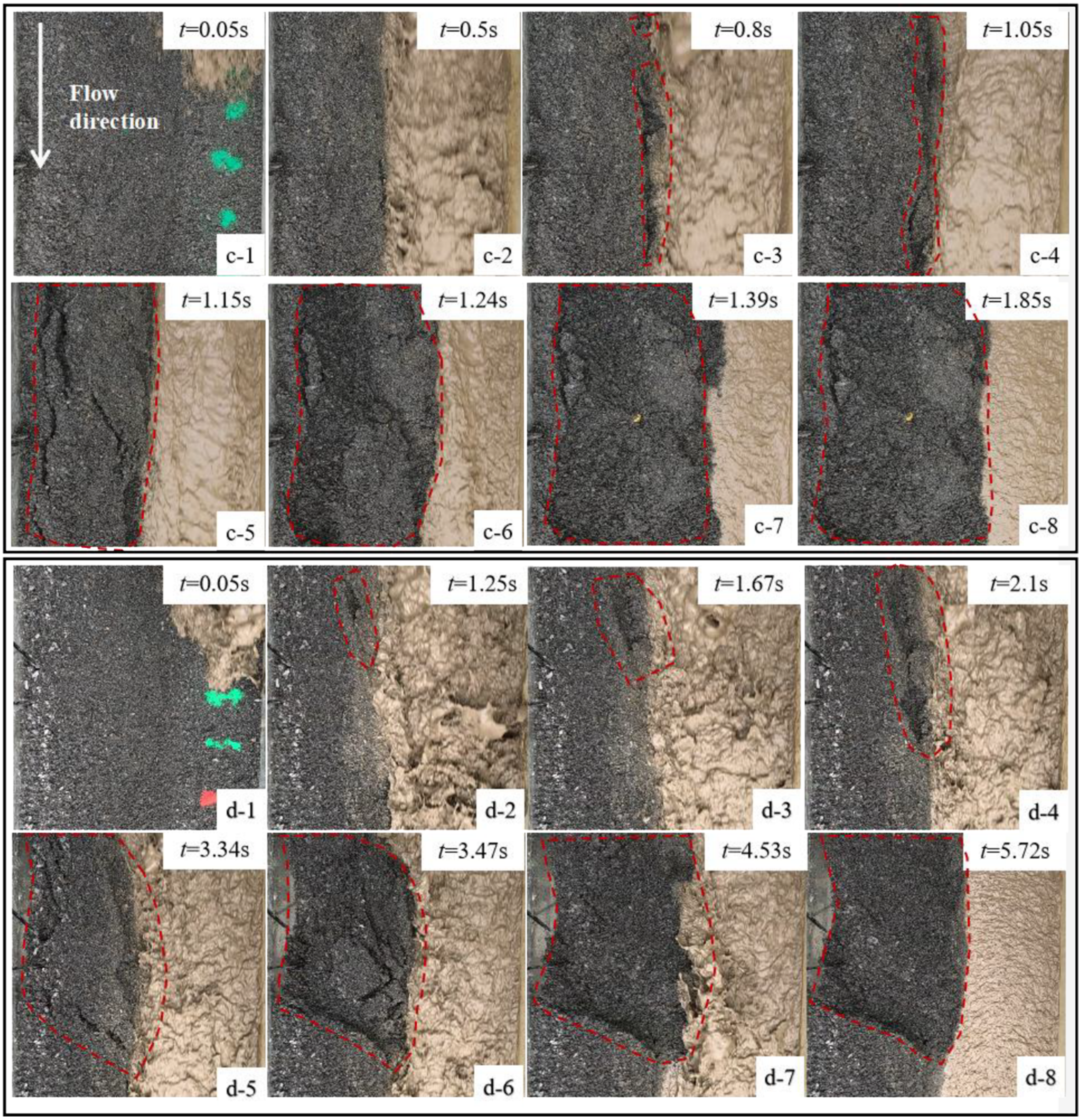

Fig. 9 (continued)

channel narrowness, and channel slope significantly impact debris flow erosion (Fig. 6). This is consistent with the previous natural debris flows (Chen et al. 2006; Rickenmann et al. 2003; Theule et al. 2015). Increased basal shear stress can lead to more erosion, while higher flow velocities and flow depths also have a significant effect on erosion. In addition, changes in bed fine particle content may alter the stability of the bed, which affects the debris flow erosion. Conversely, a stepper bed may expose debris flows to larger shear forces, further exacerbating erosion. The Froude number (F_r) is an important parameter to describe debris flow characteristics. In general, the Froude number increases as the flow velocity increases, which leads to a more chaotic flow pattern. This implies an increase in the erosive capacity of the debris flow (de Haas et al. 2022; Lyu et al. 2017).

However, we observed an unexpected trend in our experiments: as the channel narrowness increased, the Froude number (F_r) of the debris flow gradually decreased (Fig. 10).

Despite that, the erosion depth increased (Fig. 6h). This contradictory result may be due to an increase in the channel narrowness, the narrow bed restricting the lateral expansion of the debris flow, leading to an increase in the debris flow depth. Although the Fr decreases, the higher depth of the debris flow may have led to increased erosion.

The relatively minor role of grain collisional stress in controlling debris flow erosion in our experiment contrasts with observations of debris flow erosion in the field (Hsu et al. 2008, 2014; Stock and Dietrich 2006). In most studies, grain particle collision stress contributes less than 5% of the total stress (the sum of basal shear stress and particle collisional stress) (De Haas and Van Woerkom 2016), which may explain the observed relationship between downward erosion and basal shear stress, as well as the lack of a clear association between erosion and grain collision stress (Fig. 6c and d).

In summary, our results show that the debris flow regime strongly influences erosion. The debris flow regime determines the relative effects of grain collision stress and shear stress on the bed and fluid behavior (collision, friction, or viscosity). Variations in the flow regime of debris flows may explain, to some extent, the conflicting field observations of debris flow erosion (Hungr et al. 2005; Schürch et al. 2011). Changes in the flow regime of debris flows may help to explain the discrepancies between laboratory experiments and field observations (Hungr et al. 2005; Schürch et al. 2011).

Bed composition and debris flow erosion

Previous studies have clearly shown that fine particles can significantly influence debris flow erosion. It will affect the mobility of the debris flow (De Haas and Van Woerkom 2016; Iverson et al. 2011; Roelofs et al. 2022). Changes in debris flow mobility can also lead to differences in localized velocities within the debris flow. Higher localized velocities can lead to localized shearing, especially at the bed surface. Fine particles can also control the drainage conditions of the bed. Roelofs et al.'s (2022) discussion suggests that different amounts of fine particles may result in different erosion characteristics under different drainage conditions. Indeed, the effect of fine particles on bed porosity, which controls bed shearing, can significantly impact the interaction between debris flow and the bed. Localized pressure transfer defects or bed soil liquefaction in the debris flow can be induced by the reduction in bed porosity caused by fine particles. Liquefaction, in particular, can significantly influence the flow dynamics and erosion patterns. The increased pore pressure during liquefaction reduces the effective stress in the sediment, leading to a loss of strength and increased fluid-like behavior. This altered state can change erosion patterns, potentially making certain areas more susceptible to erosion.

Our studies show that bed fine particle content significantly affects debris flow erosive capacity (Fig. 6j). Adjusting the bed's fine particle content, even with minor changes, can dramatically alter the maximum DED. It may be due to (i) a decrease in grain collisional stress and (ii) an increase in viscous behavior of the debris flow with increasing bed fine particle content (De Haas et al. 2015). This suggests that when studying debris flow erosion, we should consider the complexity of the bed composition and pay attention to the bed's fine particle content. Fine particles add complexity to the bed, increase the bed cohesion, and change the bed's response to shear. Therefore, the debris flow has more complex mechanical processes when it interacts with the bed, which may reduce pore pressure (Roelofs et al. 2022). Despite that, we do not consider the changes in pore pressure since it's beyond the scope of this study.

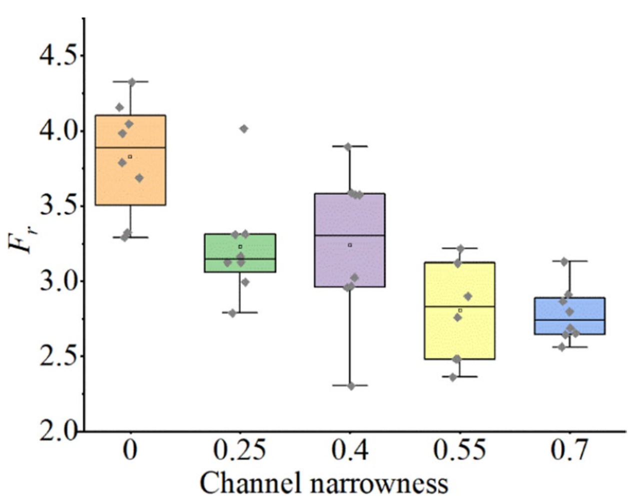

Fig. 10 The degree of bed narrowing and the Froude number

Bed morphology and debris flow erosion

Changes in bed morphology, especially variations in bed width, significantly affect debris flow erosion. Bed width directly affects the flow velocity and distribution of flow discharge. Previous studies showed that narrowing beds can increase flow velocity and concentrated flow discharge, thereby intensifying erosion (Chen et al. 2023). Specifically, higher flow velocities lead to more pronounced bed shear, while concentrated flow discharge can induce localized erosion (Knapen and Pesen 2004). On the other hand, a wider bed may lead to relatively lower flow velocities and a more extensive distribution of flow discharge, influencing debris flow erosion (Hu et al. 2013). In this case, slower flow velocities might have exerted less stress on the bed particle

(Bisschop 2018), and the dispersed flow had a more uniform erosive effect on the bed. The increase in shear stress can accelerate the abrasion of bed particles, thereby exacerbating erosion.

Lateral bed stability can also be affected by changes in the channel narrowness. Wider channels may be more effective in holding the stability of the lateral bed, reducing the potential for local collapse. In contrast, a narrower bed may increase the instability of the lateral bed, raising the risk of erosion. Localized collapses in narrower channels may lead to more concentrated erosion, exacerbating the impact on the bed. The effects of changes in the channel narrowness on debris flow erosion are multifaceted, involving interactions in fluid dynamics, bed shear stress, and local pressures.

Limitations and future work

Scale effects are crucial in debris flow model experiments (Iverson and Ouyang 2015; Iverson 2012), as small-scale setups struggle to replicate real-world conditions due to challenges in mimicking topographical variations and vegetation cover (Iverson 2012; Lyu et al. 2017). In our study, we derived parameters from field surveys to approximate transport and dynamic stress characteristics using the Froude number (Fr) and proportional length (λ) (Iverson 1997). However, replicating natural settings' complexities, like terrain variations, remains challenging (Zhou et al. 2013). Consequently, while experiments provide insights, they may not fully capture debris flow erosion attributes, requiring adjustments for practical applications. Flume tests, limited by brief durations, often fail to simulate prolonged erosion dynamics, with experimental results offering only a partial understanding of erosion mechanisms (Iverson et al. 2011). The erosion of debris flows involves a complex and extended process, where experimental outcomes typically provide only a partial understanding of the erosion mechanisms, thus falling short of capturing the holistic erosion characteristics of debris flows.

Debris flow typically shows high dynamics and complexity (Baggio et al. 2021; Berti and Simoni 2005; Breien et al. 2008). During its movement, it exhibits highly irregular flow characteristics, with the flow velocity, depth, and concentration potentially changing rapidly (de Haas et al. 2022, De Haas and Van Woerkom 2016, Egashira 1993). In narrow channels, debris flow may become more intense due to channel narrowness leading to increased flow velocity, more turbulent flow, and causing more deposition and erosion (Cantelli et al. 2004, 2007). In our study, we used the Froude number (F_r) to quantify the flow characteristics of debris flow. The F_r is an important parameter for assessing the hydrodynamic properties of fluids, but for complex fluids like debris flow, relying solely on the F_r may not fully describe their flow characteristics (Hu et al. 2012; Zhou et al. 2019). Due to the high concentration, velocity, and non-Newtonian fluid characteristics typically found in debris flow, their behavior differs significantly from open channel flow (Zhou et al. 2013). Therefore, exclusively using the F_r to quantify the flow characteristics of debris flow may have limitations and needs to be supplemented with other parameters such as concentration distribution, particle size distribution, and dynamic pressure to describe the complex flow characteristics of debris flow more accurately. In the future, novel materials like glass beads and glycerin can be utilized for testing purposes(Chen et al. 2023), enabling easy observation of changes in the internal flow field.

Conclusions

In this paper, a series of flume experiments were conducted to investigate the entrainment characteristics of debris flow with varying parameters, including bed slope, fine particle content, channel narrowness, and debris flow density. We observed different erosion patterns, which provide insights into the complex relationship between flow dynamics and channel morphology. The following conclusions are outlined:

(1) In the front of the narrow section, debris flows exhibit high flow velocity and impact force, resulting in intense erosion at the front part of the narrow section, which intensifies with the increasing narrowing. Subsequently, lateral impact erosion diminishes, giving way to lateral shear erosion as the dominant mechanism. As the debris flow advances to the middle of the narrow section, the erosion dynamics change from the front of the narrow section. Here, bed fine particles significantly influence the erosion mechanism, giving rise to distinct processes such as shear, cutting, and scouring. Less fine particles can cause overturning collapse, while more fine particles make flow depth the main factor controlling erosion.

(2) Factors affecting the DED (Downcutting erosion depth) of debris flows comprise flow velocity, depth, bed slope, and shear stress. While these variables exhibit a linear association with erosion depth, the intricate nature of debris flow and riverbed erosion processes suggests potential exponential or logarithmic relationships. The experiments that were conducted underline the significant impact of bed slope on debris flow erosion, demonstrating an increase in erosion depth with slope incline. Furthermore, the studies emphasize the significance of fine particle content in the bed, revealing a decrease in erosion depth with increased fine particle content, followed by a subsequent increase past a certain threshold. As channel narrowness expands, the DED initially inclines, then declines, reaching a mini-

mum at channel narrowness of 0.25, indicating fluctuations related to cross-sectional area and flow dynamics.

(3) We introduce the parameter of erosion efficiency, which is calculated as the sum of the vertical incision rate and lateral erosion rate, to assess the erosion capacity of debris flow. The effects of significant factors like bed slope, bed fine particle content, debris flow density, and channel narrowness on Es were thoroughly investigated. A rise in bed slope escalates erosion efficiency, whereas an increase in fine particle content diminishes it. As channel narrowness decreases, erosion efficiency exhibits an exponential growth trend due to the turbulent flow regime within narrow channels.

(4) A dimensionless parameter, ξ, is introduced to signify the relative significance of lateral and vertical erosion in debris flow. As debris flow density and bed slope rise, ξ decreases, indicating an increased downward erosion tendency. The influence of bed fine particle content on ξ is found to be minimal. Overall, ξ demonstrates logarithmic escalation as channel narrowness increases, underlining its pivotal role in debris flow erosion. At narrower channels, lateral erosion prevails, while at wider channels, vertical erosion becomes dominant. These observations offer valuable insights into the erosion dynamics of debris flows.

Supplementary Information The online version contains supplementary material available at https://doi.org/10.1007/s10064-024-03742-6.

Acknowledgements The study is financially supported by the National Key R&D Program of China (2018YFC1505205), Key Research and Development, Program of Tibet Autonomous Region (XZ202301ZY0039G), the Science and Technology Research Program of the Institute of Mountain Hazards and Environment, Chinese Academy of Sciences (IMHE-ZDRW-01).

Data availability All raw data can be provided by the corresponding authors upon request.

Declarations

Competing interest The authors declare that they have no known competing financial interests or personal relationships that could have appeared to influence the work reported in this paper.

References

Al-Riffai M (2014) Experimental study of breach mechanics in overtopped noncohesive earthen embankments. Université d'Ottawa/University of Ottawa

Baggio T, Mergili M, D'agostino V 2021. Advances in the simulation of debris flow erosion: the case study of the Rio Gere (Italy) event of the 4th August 2017. Geomorphology [J] 381:107664

Berger C, McArdell B, Schlunegger F (2011) Direct measurement of channel erosion by debris flows, Illgraben, Switzerland. J Geophys Res: Earth Surface 116. https://doi.org/10.1029/2010JF001722

Berti M, Simoni A (2005) Experimental evidences and numerical modelling of debris flow initiated by channel runoff. Landslides 2:171–182. https://doi.org/10.1007/s10346-005-0062-4

Berti M, Genevois R, Simoni A, Tecca PR (1999) Field observations of a debris flow event in the Dolomites. Geomorphology 29:265–274. https://doi.org/10.1016/S0169-555X(99)00018-5

Bisschop F (2018) Erosion of sand at high flow velocities: an experimental study

Borrelli P, Robinson DA, Panagos P, Lugato E, Yang JE, Alewell C, Wuepper D, Montanarella L, Ballabio C (2020) Land use and climate change impacts on global soil erosion by water (2015–2070). Proc Natl Acad Sci 117:21994–22001. https://doi.org/10.1073/pnas.2001403117

Breien H, De Blasio FV, Elverhøi A, Høeg K (2008) Erosion and morphology of a debris flow caused by a glacial lake outburst flood, Western Norway. Landslides 5:271–280. https://doi.org/10.1007/s10346-008-0118-3

Cantelli A, Paola C, Parker G (2004) Experiments on upstream-migrating erosional narrowing and widening of an incisional channel caused by dam removal. Water Resour Res [J] 40:n/a-n/a

Cantelli A, Wong M, Parker G, et al. (2007) Numerical model linking bed and bank evolution of incisional channel created by dam removal. Water Resour Res [J] 43

Chang D, Zhang L, Xu Y, Huang R (2011) Field testing of erodibility of two landslide dams triggered by the 12 May Wenchuan earthquake. Landslides 8:321–332. https://doi.org/10.1007/s10346-011-0256-x

Chen H, Crosta G, Lee C (2006) Erosional effects on runout of fast landslides, debris flows and avalanches: a numerical investigation. Geotechnique 56:305–322. https://doi.org/10.1680/geot.2006.56.5.305

Chen Q, Song D, Chen X et al (2023) Visco-collisional scaling law of flow resistance and its application in debris-flow mobility. J Geophys Res: Earth Surface [J] 128:e2022JF006712

Chigira M, Wu X, Inokuchi T, Wang G (2010) Landslides induced by the 2008 Wenchuan earthquake, Sichuan, China. Geomorphology 118:225–238. https://doi.org/10.1016/j.geomorph.2010.01.003

Croissant T, Lague D, Steer P, Davy P (2017) Rapid post-seismic landslide evacuation boosted by dynamic river width. Nat Geosci 10:680–684. https://doi.org/10.1038/ngeo3005

Curran JC, Coveleski KC (2021) How sediment composition and flow rate influence downstream channel morphodynamics upon dam removal. Earth Surf Proc Land 46:2437–2447. https://doi.org/10.1002/esp.5187

De Haas T, Braat L, Leuven JR, Lokhorst IR, Kleinhans MG (2015) Effects of debris flow composition on runout, depositional mechanisms, and deposit morphology in laboratory experiments. J Geophys Res Earth Surf 120:1949–1972. https://doi.org/10.1002/2015JF003525

De Haas T, Van Woerkom T (2016) Bed scour by debris flows: experimental investigation of effects of debris-flow composition. Earth Surface Process Landforms 41. https://doi.org/10.1002/esp.3963

de Haas T, McArdell B, Nijland W, Åberg A, Hirschberg J, Huguenin P (2022) Flow and bed conditions jointly control debris-flow erosion and bulking. Geophys Res Lett e2021GL097611. https://doi.org/10.1029/2021GL097611

Egashira S, Ashida K (1987) Sediment transport in steep slope flumes. Proc. RoC Japan Joint Seminar on Water Resources

Egashira S (1993) Mechanism of sediment deposition from debris flow (part 1). J Japan Soc Erosion Control Eng [J] 46:186

Gao, GS, et al (2006) Application of piv method to determine debris flow velocity. Soil Water Conserv Appl Technol 6. https://doi.org/10.3969/j.issn.1673-5366.2006.06.002 (in Chinese)

Godt JW, Coe JA (2007) Alpine debris flows triggered by a 28 July 1999 thunderstorm in the central front range, Colorado. Geomorphology 84:80–97. https://doi.org/10.1016/j.geomorph.2006.07.009

Han Z, Chen G, Li Y, Tang C, Xu L, He Y, Huang X, Wang W (2015a) Numerical simulation of debris-flow behavior incorporating a dynamic method for estimating the entrainment. Eng Geol 190:52–64. https://doi.org/10.1016/j.enggeo.2015.02.009

Han Z, Chen G, Li Y, et al (2015) Exploring the velocity distribution of debris flows: an iteration algorithm based approach for complex cross-sections[J].Geomorphology 241(jul.15):72–82. https://doi.org/10.1016/j.geomorph.2015.03.043

Hsu Y, Yen H, Tseng W, Jan C (2014) Numerical simulation on a tremendous debris flow caused by typhoon Morakot in the Jiaopu Stream, Taiwan. J Mountain Sci 11:1–18. https://doi.org/10.1007/s11629-013-2754-x

Hsu L, Dietrich WE, Sklar LS (2008) Experimental study of bedrock erosion by granular flows. J Geophys Res: Earth Surface 113. https://doi.org/10.1029/2007jf000778

Hu K, Cui P, Zhang J (2012) Characteristics of damage to buildings by debris flows on 7 August 2010 in Zhouqu, Western China. Nat Hazards Earth Syst Sci [J] 12:2209–2217

Hu K, Tian M, Li Y (2013) Influence of flow width on mean velocity of debris flows in wide open channel. J Hydraul Eng 139:65–69. https://doi.org/10.1061/(ASCE)HY.1943-7900.0000648

Hu K, Ge Y, Cui P, Guo X, Yang W (2011) A preliminary study of the mudslide disaster in Zhouqu, Gansu. 2010. Preliminary understanding of the Zhouqu mega-debris flow disaster in Gansu. J Mountain Geol 28:628–634. https://doi.org/10.16089/j.cnki.1008-2786.2010.05.012 (**in Chinese**)

Hungr O, Morgan G, Kellerhals R (1984) Quantitative analysis of debris torrent hazards for design of remedial measures. Can Geotech J 21:663–677. https://doi.org/10.1139/t84-073

Hungr O, McDougall S, Bovis M (2005) Entrainment of material by debris flows. Debris-flow hazards and related phenomena. Springer 135–158

Iverson RM (1997) The physics of debris flows. Rev Geophys 35:245–296. https://doi.org/10.1029/97RG00426

Iverson RM, Ouyang CJ (2015) Entrainment of bed material by Earth-surface mass flows: review and reformulation of depth-integrated theory. Rev Geophys [j] 53:27–58

Iverson RM, Reid ME, LaHusen RG (1997) Debris-flow mobilization from landslides. Annu Rev Earth Planet Sci 25:85–138. https://doi.org/10.1146/annurev.earth.25.1.85

Iverson RM, Reid ME, Logan M, LaHusen RG, Godt JW, Griswold JP (2011) Positive feedback and momentum growth during debris-flow entrainment of wet bed sediment. Nat Geosci 4:116–121. https://doi.org/10.1038/ngeo1040

Iverson, RM 2012. Elementary theory of bed-sediment entrainment by debris flows and avalanches. Journal of Geophysical Research: Earth Surface [J], 117.

Jakob M, Hungr O, Hungr O (2005) Classification and terminology. Debris-flow hazards and related phenomena [J]: 9–23

Kaitna R, Dietrich W, Hsu L (2014) Surface slopes, velocity profiles and fluid pressure in coarse-grained debris flows saturated with water and mud. J Fluid Mech 741:377–403

Knapen AUJC, Poesen JUJ (2004) Resistance of topsoils to concentrated flow erosion: a review of the available experimental data. international symposium on gully erosion edition:3rd location:Oxford, Mississippi date:April 28-May 1, 2004

Li P, Hu K, Wang X (2018) Debris flow entrainment rates in non-uniform channels with convex and concave slopes. J Hydraul Res 56:156–167. https://doi.org/10.1080/00221686.2017.1313321

Liu J, Nakatani K, Mizuyama T (2013) Effect assessment of debris flow mitigation works based on numerical simulation by using Kanako 2D. Landslides 10:161–173. https://doi.org/10.1007/s10346-012-0316-x

Lyu L, Wang Z, Cui P, Xu M (2017) The role of bank erosion on the initiation and motion of gully debris flows. Geomorphology 285:137–151

Lyu L, Wang Z, Cui P, Xu M (2018) Influence of lateral erosion of gully banks on unsteady dynamic processes of debris flows. Adv Water Sci 29:213–220

Mangeney A, Roche O, Hungr O, Mangold N, Faccanoni G, Lucas A (2010) Erosion and mobility in granular collapse over sloping beds. J Geophys Res: Earth Surface 115. https://doi.org/10.1029/2009JF001462

McDougall S, Hungr O (2005) Dynamic modelling of entrainment in rapid landslides. Can Geotech J 42:1437–1448. https://doi.org/10.1139/t05-064

Ning L, Hu K, Wang Z, Luo H, Qin H, Zhang X, Liu S (2022) Multi-hazard chain reaction initiated by the 2020 Meilong debris flow in the Dadu River, Southwest China. Front. Integ Dis Risk Manag: From Earth Sci Policy Making 10:142

Patalano A, García CM, Rodríguez A (2017) Rectification of Image Velocity Results (RIVeR): a simple and user-friendly toolbox for large scale water surface Particle Image Velocimetry (PIV) and Particle Tracking Velocimetry (PTV). Comput Geosci 323–330

Prochaska AB, Santi PM, Higgins JD, Cannon SH (2008) A study of methods to estimate debris flow velocity. Landslides 5:431–444. https://doi.org/10.1007/s10346-008-0137-0

Rickenmann D, Weber D, Stepanov B (2003) Erosion by debris flows in field and laboratory experiments. International conference on debris-flow hazards mitigation: mechanics, prediction, and assessment, proceedings 883–894

Roelofs L, Colucci P, de Haas T (2022) How debris-flow composition affects bed erosion quantity and mechanisms: an experimental assessment. Earth Surf Proc Land 47:2151–2169. https://doi.org/10.1002/esp.5369

Savage SB, Hutter K (1989) The motion of a finite mass of granular material down a rough incline. J Fluid Mech 199:177–215. https://doi.org/10.1017/S0022112089000340

Stock JD, Dietrich WE (2006) Erosion of steepland valleys by debris flows. Geol Soc Am Bull 118:1125–1148. https://doi.org/10.1130/B25902.1

Schürch P, Densmore AL, Rosser NJ et al (2011) Detection of surface change in complex topography using terrestrial laser scanning: application to the Illgraben debris-flow channel. Earth Surf Process Landf [J] 36:1847–1859

Takahashi T (1981) Debris flow. Annu Rev Fluid Mech 13:57–77. https://doi.org/10.1146/annurev.fl.13.010181.000421

Theule J, Liébault F, Laigle D, Loye A, Jaboyedoff M (2015) Channel scour and fill by debris flows and bedload transport. Geomorphology 243:92–105. https://doi.org/10.1016/j.geomorph.2015.05.003

Wang Z (2008) A preliminary report on the great Wenchuan earthquake. Earthq Eng Eng Vib 7:225–234. https://doi.org/10.1007/s11803-008-0856-1

Whipple KX, Dunne T (1992) The influence of debris-flow rheology on fan morphology, Owens Valley, California. Geol Soc Am Bull 104:887–900. https://doi.org/10.1130/0016-7606(1992)104%3c0887:TIODFR%3e2.3.CO;2

Yong C, Booth DC, Yong C, Booth DC (2011) The Wenchuan earthquake. Springer

Zhang S, Zhang L (2017) Impact of the 2008 Wenchuan earthquake in China on subsequent long-term debris flow activities in the epicentral area. Geomorphology 276:86–103. https://doi.org/10.1016/j.geomorph.2016.10.009

Zhang ZL, Xie J, Yu DK, Wen ZJ (2019) Analysis of a debris flow after Wenchuan earthquake and discussion on preventive measures. Therm Sci 23:1563–1570. https://doi.org/10.2298/TSCI180811224Z

Zhou GG, Cui P, Chen H et al (2013) Experimental study on cascading landslide dam failures by upstream flows. Landslides [j] 10:633–643

Zhou GG, Zhou M, Shrestha MS et al (2019) Experimental investigation on the longitudinal evolution of landslide dam breaching and outburst floods. Geomorphology [j] 334:29–43